

Calculating Pressure Concentration Factors In Keyless Locking Assemblies

Sandro Zamboni and Massimiliano Margonari, MAV S.p.A.



Figure 1—The MAV 1008, 4061, 2005 and 1061 keyless locking assemblies.

Introduction

One of the most important goals for designers and producers of mechanical components is to supply customers increasingly high quality products with clearly defined performance expectations. For this purpose, MAV S.p.A., an established manufacturer of locking assemblies and shrink disks, began to explore several years ago the methods of computer simulation to improve the components in production and to support the design process. This has substantially reduced laboratory testing, limiting its use to simply validating certain configurations, resulting in a significant reduction in times and costs for the certification of new products.

There are a wide number of different reasons that led the MAV engineering division to make this decision. Firstly, there is the management's belief that investing in applied research and numerical simulation is an effective means to ensure the

best possible results at the least possible cost, with obvious advantages; secondly, there is the growing technical need for fast, reliable and accurate instruments to offer the best possible response to the demands of the market.

The technical data of most interest to the mechanical engineer designing a locking assembly are usually the values for maximum transmissible torsional and flexural moments. Once the geometry, friction coefficients between the surfaces and the pre-tightening torque applied to the screws have been established, these values may be calculated using a number of equations formulated on the basis of simplified models, which are widely accepted and used by engineers. The results obtained are always safety biased; the mathematical models used often provide transmissible moment values well below the real capabilities of the system, as demonstrated by a series of tests conducted by MAV on a variety of different products.

It is useful to know the distribution of contact pressure between the locking assembly and the shaft throughout the system's life cycle and, in particular, during assembly and certain operating conditions. Unfortunately, there are no simplified models to help provide indications on the distribution of tension generated by the locking assembly on the mechanical components that it connects. In fact, no laboratory test currently exists that is capable of giving even partial answers to these questions. Literature cites the results obtained in the early 1980s and a number of indications on the matter. These results were obtained via the finite element analysis of extremely simplified, axially symmetric models, probably because of the limitations of the hardware and software resources available at the time.

However, while the data obtainable from two-dimensional simulation models may undoubtedly be interesting, and MAV has also made use of this technique, they do not provide any information on the behavior of locking assemblies near the gaps in the rings, where peak tensions are expected.

The accurate determination of con-

tact pressure distribution is no small matter. Knowing the position and intensity of any tension peaks facilitates the job of the engineer, who will thus be able to make full use of the mechanical capabilities of the system in question while still maintaining adequate safety levels. To shed more light on this aspect, MAV has conducted a detailed study, using an entirely numerical approach, to produce more precise and reliable data concerning the real distribution of forces generated on a shaft by a locking assembly. The study considered the MAV 1008, 4061, 2005 and 1061 series of products. For each series, four different shaft sizes were considered to give the broadest and most detailed vision possible. The study also developed three-dimensional models with extremely accurate geometrical representation. The resulting models were highly complex and demanding in terms of computing power.

How a Locking Assembly Works

Figures 1 and 2 illustrate the four different types of locking assembly considered for this study. Tables 1 and 2 also

contain pertinent information concerning geometry, the screws used and the theoretical reference values for contact pressure obtained with simplified models. The operating principle for a locking assembly is rather simple: a number of conical section rings are brought together by tightening screws, which generates high contact pressures between the shaft, the hub and the locking assembly itself. This arrangement holds the components tightly together, enabling the transmission of torque. The rings in contact with the shaft and the hub always have a longitudinal gap to reduce their circumferential rigidity, facilitating and improving the elimination of free play between components.

The locking assembly is usually mounted on the shaft and the screws pre-tightened in the tried and tested criss-cross sequence to limit possible eccentricity in the final configuration. The hub is mounted outside the locking assembly and enables the transmission of torque. The hub must be appropriately

continued

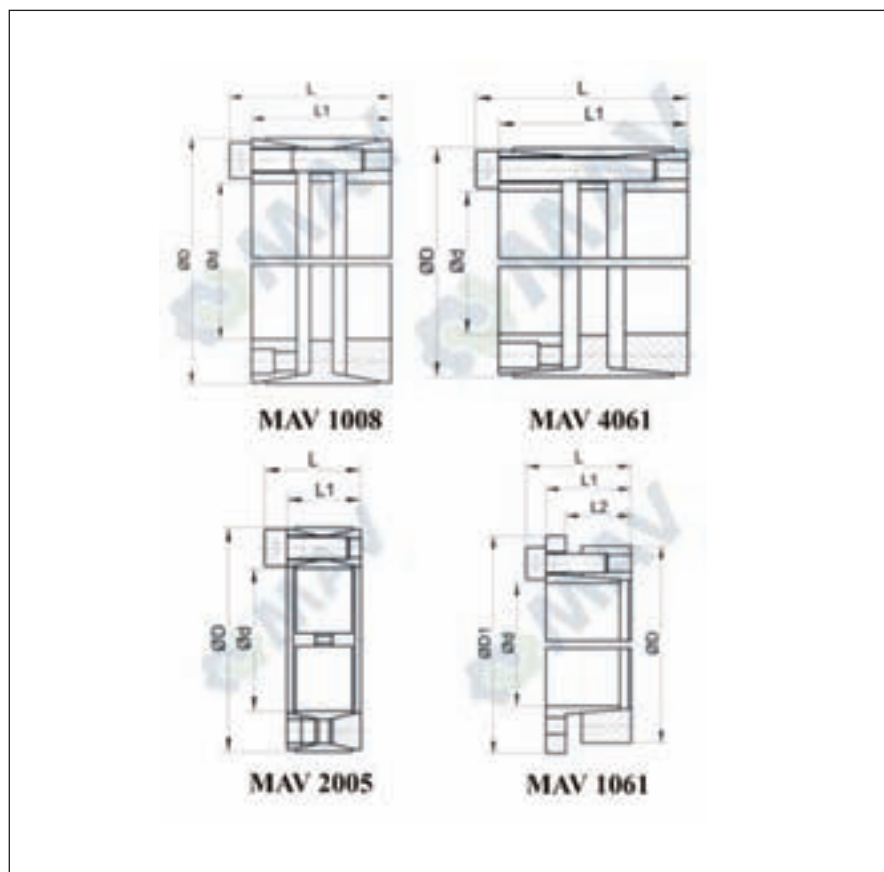


Figure 2—Longitudinal cross-sections of the MAV 1008, 4061, 2005 and 1061 locking assemblies, indicating the most significant dimensions.

**Table 1—Dimensions of Locking Assemblies and Hubs Used in the Study.
The Shaft Diameter is Equal to the Interior Diameter (d) of the Locking Assembly.**

	Dimensions (mm)						Hub	
	Locking Assembly							
MAV 1008	d	D	L	L1			External diameter	Depth
70 x 110	70	110	74	66			150	60
100 x 145	100	145	114	102			300	100
200 x 260	200	260	165	149			450	140
400 x 495	400	495	225	203			900	200
MAV 4061	d	D	L	L1			External diameter	Depth
50 x 80	50	80	74	66			150	60
100 x 145	100	145	114	102			300	100
200 x 260	200	260	165	149			450	140
400 x 495	400	495	225	203			900	200
MAV 2005	d	D	L	L1			External diameter	Depth
50 x 80	50	80	32	24			150	28
100 x 145	100	145	45	33			360	40
200 x 260	200	260	66	52			580	58
400 x 495	400	495	112	90			990	100
MAV 1061	d	D	D1	L2	L1	L	External diameter	Depth
50 x 80	50	80	89	27	35	43	150	27
100 x 145	100	145	154	33	45	57	290	33
200 x 260	200	260	269	51	65	79	480	51
400 x 495	400	495	504	94	116	138	910	94

Table 2—Type and Number of Screws Used with Locking Assemblies Considered in Study.

	Screws (class 12.9) Number and Type	Mean theoretical pressure (MPa)		Maximum Theoretical Transmissible Torque (N-mm)
		On shaft	On Hub	
MAV 1008				
70 x 110	8 M10	197	125	7280•10 ³
100 x 145	10 M12	215	148	19400•10 ³
200 x 260	18 M14	166	128	95300•10 ³
400 x 495	22 M22	168	136	609500•10 ³
MAV 4061				
50 x 80	8 M8	198	124	4120•10 ³
100 x 145	11 M12	210	145	27700•10 ³
200 x 260	16 M16	181	139	149900•10 ³
400 x 495	24 M22	188	152	863900•10 ³
MAV 2005				
50 x 80	12 M8	282	176	2160•10 ³
100 x 145	14 M12	307	214	11690•10 ³
200 x 260	30 M14	254	195	65450•10 ³
400 x 495	36 M22	218	176	393360•10 ³
MAV 1061				
50 x 80	7 M8	191	119	1800•10 ³
100 x 145	8 M12	206	142	10100•10 ³
200 x 260	15 M14	153	118	50900•10 ³
400 x 495	21 M22	146	118	377900•10 ³

sized to effectively oppose any radial deformity of the locking assembly and may, for reasons of space but also for aesthetic or cost reasons, also incorporate drums, gear wheels or any other mechanical component deemed necessary.

Once the pre-tightening torque for the screws has been applied, the system consists of parts solidly connected to one another and may be subjected to external loads. The MAV 1008 and 2005 are defined as self-releasing locking assemblies. If the screws are removed after fitment of the locking assembly, they tend to loosen and return to their initial undeformed configuration. This is due to the fact that the rings have a highly conical section (8, 10°), and the coefficient of friction, usually considered to be 0.12, is not high enough to keep the components in the deformed configuration. This is an extremely desirable characteristic, as the locking assembly may be mounted and removed numerous times during its life cycle. Conversely, the MAV 4061 and 1061 are known as self-locking components. With a conical section of less than 5°, these exhibit the opposite behavior of that described above. In this case, the screws perform no particular structural role and serve only to deform the rings sufficiently.

As can easily be understood, the pressure generated on the shaft is not uniformly distributed (which would be considered an ideal condition) and varies both longitudinally and circumferentially due to the varying rigidity of the holes of the rings constituting the locking assembly (see examples in Figures 7 and 8). Furthermore, as mentioned previously, contact between the gaps in the rings and the shaft and hub constitutes a substantial element of disturbance and can cause undesirable tension peaks. This is why three-dimensional modeling was chosen, focusing on zones of discontinuity, such as edges and gaps in the rings.

CAD Models

Autodesk Inventor 10 software was used to produce the three-dimensional models of the locking assemblies considered. The capability of the software to parameterize the geometries modeled was extensively

continued

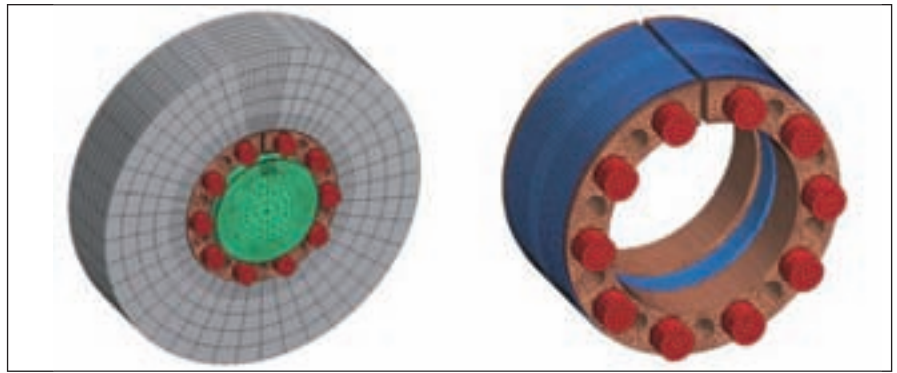


Figure 3—Meshes of the MAV 1008 100 x 145 locking mechanism, of the shaft and hub (left) and of the locking mechanism alone (right).

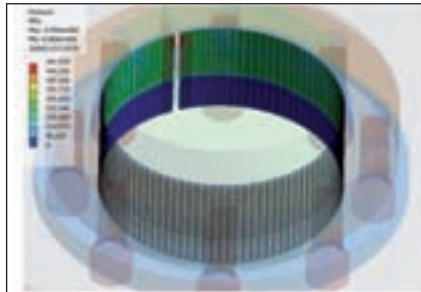


Figure 4—MAV 1061 100 x 145, shaft-locking assembly contact pressure on locking assembly at the end of the screw tightening stage. Note the concentration of pressure near the gap, at the front zone of the flange.

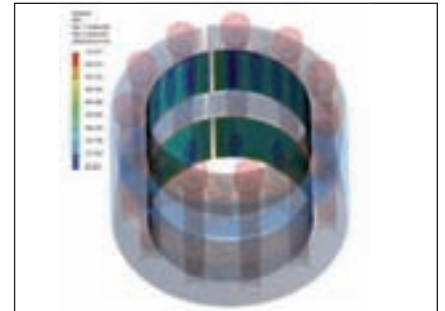


Figure 5—MAV 4061 100 x 145, shaft-locking assembly contact pressure on locking assembly at the end of load application. Note the reduction in contact pressure near the ring holes.

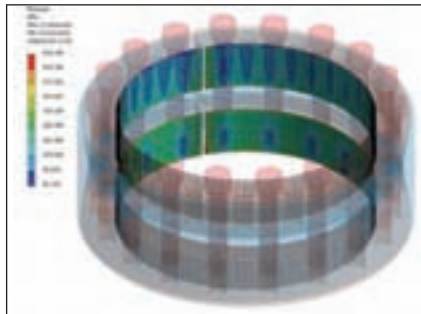


Figure 6—MAV 1008 200 x 260, shaft-locking assembly contact pressure on locking assembly at the end of the screw tightening stage. In this case there are two concentrations of contact pressure located at the front zones of the two rings, in correspondence with the gaps.

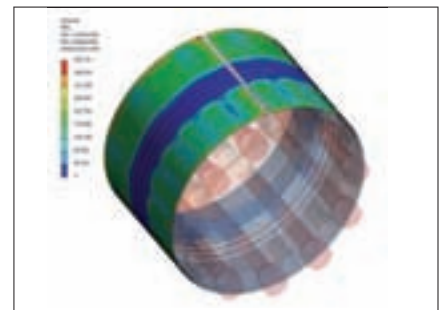


Figure 7—MAV 4061 100 x 145, hub-locking assembly contact pressure on locking assembly at the end of load application. Note the circumferential zone in correspondence with the flange, where contact pressures are very low and, in some cases, nil.

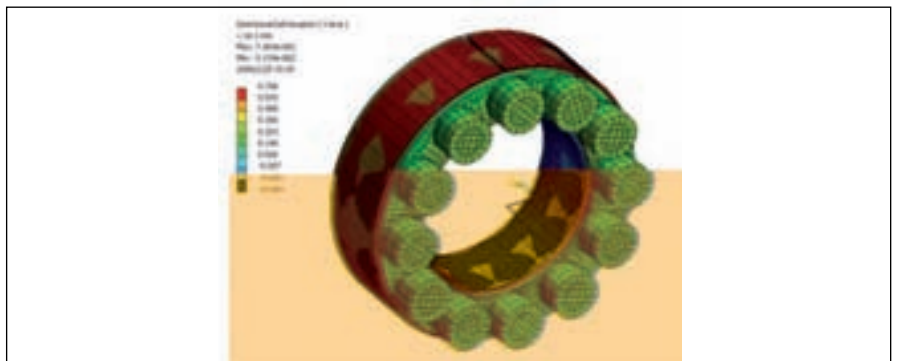


Figure 8—MAV 2005 50 x 80, radial displacement of the locking assembly at the end of the pre-tightening stage. The inner ring closes onto the shaft while the outer ring opens onto the hub.

exploited to speed up the preparation of the models themselves. While this required more work than usual procedures, it permitted the analysis of additional measurements when deemed necessary, without requiring significant extra effort. Painstaking care went into modeling, bearing in mind from the start of the procedure that the geometries created would subsequently have to be processed by a finite element mesher. In particular, a substantial “defeaturing” process was applied to the geometries to minimize the number of nodes and small surfaces that do not contribute significantly to the definition of elements and do not influence structural response. This presented clear advantages during mesh construction. The external surfaces of all components were subdivided into as uniformly shaped quadrilaterals as possible, permitting a

more uniform subsequent meshing process, especially in contact areas.

The IGES format was chosen to facilitate transfer of the geometries into the finite element simulation environment.

FEM Models

Ansys 10.0 software was used for the numerical simulations. In particular, the Workbench environment was used for the preparation of the models and the visualization of the results, whereas the batch launch was conducted on a Linux machine for the actual analyses. Only elements with quadratic form functions were used and the ‘Hex Dominant’ setting was enabled to ensure greater mesh uniformity, as this reduces the number of nodes used and achieves better results than other settings. ‘Weak springs’ were also used to prevent rigid behavior in certain parts of the model. The very low

rigidity of these springs enabled a solution to be reached without significantly altering the response of the system. Table 3 indicates the number of nodes and elements and the degrees of freedom for each individual model. Note that the number of contact and target contact elements are always identical in each model. This is because symmetrical contact definition was always employed. Managing the contact elements is fundamental; augmented Lagrangian formulation methods were always used, monitoring penetration occurring between bodies and modifying the parameters in successive instances where necessary. A coefficient of friction of 0.12 was chosen, as this value was considered sufficiently low and statistically reliable for describing steel-steel contact. The material, which is identical in all parts involved, was con-

Table 3—Finite Element Models: Nodes, Elements and Degrees of Freedom Applied in Analyses.

Model	Nodes	d.o.fs	Elements				
			SOLID 186-187	CONTA 174	TARGE 170	PRETS 179	COMBIN 14
MAV 1008							
70 x 110	292,537	887,601	79,293	15,135	15,135	8	312
100 x 145	360,336	1,080,994	97,643	20,724	20,724	10	360
200 x 260	425,297	1,275,861	51,458	25,729	25,729	18	552
400 x 495	462,964	1,388,854	127,141	29,925	29,925	22	648
MAV 4061							
50 x 80	314,089	942,257	87,281	15,168	15,168	8	312
100 x 145	351,697	1,055,075	96,304	21,457	21,457	11	384
200 x 260	411,116	1,233,322	110,871	27,683	27,683	16	504
400 x 495	450,338	1,350,972	121,679	27,785	27,785	24	696
MAV 2005							
50 x 80	356,263	1,068,771	104,024	17,495	17,495	12	432
100 x 145	366,645	1,099,913	105,956	18,584	18,584	14	480
200 x 260	299,780	899,268	82,701	19,033	19,033	30	864
400 x 495	528,261	1,584,717	149,978	32,658	32,658	36	1008
MAV 1061							
50 x 80	207,692	623,071	59,031	11,109	11,109	7	264
100 x 145	240,670	722,003	68,132	13,607	13,607	8	288
200 x 260	436,743	1,310,208	122,083	23,614	23,614	15	456
400 x 495	587,715	1,763,112	166,613	32,675	32,675	21	600

sidered to be a linearly elastic isotropic material, with a Young modulus of 200 GPa and a Poisson coefficient of 0.3. The only non-linearity considered in the models is due to the presence of contact points with friction. Certain analyses conducted in the past have shown that including other non-linearities, such as plasticity or large-scale deformation and large-scale movement, introduces no advantages in terms of the quality of the results for locking assembly shaft contact pressures and significantly increases calculation times.

Contact Pressure Concentration Factors

The primary objective of this study is to identify a simplified quantity for use during the design stage that is sufficiently representative of the state of tension induced on the shaft by the locking assembly. The following formula is often defined for this purpose:

$$FCP = \frac{p_{max}}{p_m} \quad (1)$$

where FCP is the Contact Pressure Factor and p_{max} and p_m are, respectively, maximum and mean contact pressure.

This is calculated with the following equation:

$$p_m = \frac{\int_{A_c, \text{if } p(x) > 0} p(x) \, dAx}{\int_{A_c, \text{if } p(x) > 0} dAx} \quad (2)$$

where $p(x)$ is the contact pressure at point x on surface A_c . Obviously, in the calculation of the integrals given above, only the area where contact pressure is not nil following the application of loads is considered, not the initial contact surface. We must also remember that the contact surface between bodies is generally not known beforehand and depends, obviously, on the deformation modes of the structure.

$$F_R = \int_{A_c, \text{if } p(x) > 0} p(x) \, dAx \quad (3)$$

Equation 3 represents the radial force transmitted from the locking assembly

continued

Table 4—Mean Contact Pressures Determined at Each Load Step, for Each Measurement and for Each Series of Locking Assembly Considered.

Mean Contact Pressures (MPa)				
MAV 1008				
Load Step	70 x 110	100 x 145	200 x 260	4000 x 495
1	194.4	214.2	183.0	182.9
2	198.9	219.8	185.8	185.3
3	200.0	220.2	185.9	185.8
4	200.5	220.4	186.2	185.9
5	200.6	220.7	186.7	186.2
6	200.8	221.1	186.6	186.4
MAV 4061				
Load Step	50 x 80	100 x 145	200 x 260	400 x 495
1	196.1	208.8	230.7	201.3
2	198.4	211.0	230.6	201.8
3	198.1	211.0	230.3	202.2
4	198.0	210.5	230.1	202.3
5	198.0	210.5	230.2	202.4
6	198.4	210.5	230.4	202.5
MAV 2005				
Load Step	50 x 80	100 x 145	200 x 260	400 x 495
1	259.0	250.4	246.8	193.5
2	263.3	252.1	248.8	194.9
3	264.2	252.6	250.5	195.5
4	265.3	253.1	250.8	195.7
5	266.3	253.5	251.3	196.0
6	267.8	253.3	252.0	196.3
MAV 1061				
Load Step	50 x 80	100 x 145	200 x 260	400 x 495
1	192.5	193.4	152.6	150.2
2	193.6	193.0	152.6	150.2
3	193.6	194.8	152.4	153.2
4	193.2	194.8	152.7	152.6
5	192.5	194.6	152.1	152.8
6	187.2	193.8	152.3	153.6

Table 5—Mean Contact Pressures (FCP) Determined at Each Load Step, for Each Measurement and for Each Series of Locking Assembly Considered.				
Contact Pressure Concentration Factors (FCP)				
MAV 1008				
Load Step	70 x 110	100 x 145	200 x 260	4000 x 495
1	2.1	2.1	1.9	1.9
2	2.3	2.3	2.2	2.1
3	2.3	2.2	2.0	2.1
4	2.3	2.2	2.0	2.1
5	2.3	2.1	2.0	2.1
6	2.3	2.2	2.0	2.1
MAV 4061				
Load Step	50 x 80	100 x 145	200 x 260	400 x 495
1	2.6	2.1	2.0	2.0
2	3.2	2.8	2.2	1.9
3	2.9	2.6	2.1	1.8
4	2.9	2.5	2.1	1.8
5	2.8	2.5	2.1	1.9
6	2.8	2.5	2.1	2.0
MAV 2005				
Load Step	50 x 80	100 x 145	200 x 260	400 x 495
1	1.6	1.9	1.4	1.6
2	1.6	1.9	1.4	1.6
3	1.8	2.0	1.6	1.7
4	1.9	2.1	1.6	1.8
5	2.0	2.2	1.7	1.9
6	2.3	2.3	1.8	2.0
MAV 1061				
Load Step	50 x 80	100 x 145	200 x 260	400 x 495
1	2.8	2.3	2.0	1.4
2	2.9	2.5	2.2	1.5
3	3.3	2.9	2.7	1.7
4	3.4	3.0	2.8	1.8
5	3.5	3.2	2.9	2.0
6	3.7	3.3	3.1	2.0

to the shaft and to the hub. In this study, Equation 1 was not used because it is not considered sufficiently representative in this context. Instead, a modified version of the formula was proposed, as described as follows.

It is known that in finite element analysis, when a linear elastic behavior is attributed to the material, there are no limits to stress values attainable within the bodies. Where there are concentrated forces, sharp corners or contact between parts, the values for the state of tension in some nodes may increase indefinitely and congest the calculation mesh. This is a logical consequence of the fact that elastostatic equations permit the non-definition of the tension state in certain points in space; a well-known example of this is the Boussinesq problem, to which there is an analytical solution.

However, the integral of the state of tension calculated for a finite domain that also includes singularities is well defined and represents the result of the applied forces. In the case of a locking assembly, the transmitted radial force (Eq. 3) always assumes finite values, even though there are points in which the contact pressure $p(x)$ is not defined or, in the case of an FEM model, increases indefinitely to congest the mesh.

For this reason, the following definition was introduced:

$$FCP = \frac{p_{perc}}{p_m} \quad (4)$$

where p_{perc} is a pressure value not known beforehand, representing the pressure at which the majority of the radial force (in our case 99.75%) is transmitted.

The value of p_{perc} may be calculated with the following equation:

$$perc F_R = \int_{A_c, \text{ if } p(x) > 0} p(x) dAx \quad (5)$$

where $perc$ is a real number slightly less than unity (in our case 0.9975). Thus, the value p_{perc} , which is independent of the calculation mesh (as demonstrated in a separate study), is sufficiently representative of the pressure concentration. It is important to note, however, that the FCP only considers the normal component of

the state of strain at the contact surface and, therefore, cannot provide exhaustive information regarding the effective state of tension.

Another limit consists in the fact that the *FCP* provides no description of stress distribution, which is important in evaluating whether a situation is dangerous or not. For operational purposes, it was decided to consider the pressure at the centroid of the contact elements. Mean pressure is therefore:

$$p_m = \frac{\sum_{e = \text{lif } p(e) > 0}^{N_e} p_e A_e}{\sum_{e = \text{lif } p(e) > 0}^{N_e} A_e} \quad (6)$$

where N_e represents the number of elements considered while p_e and A_e represent, respectively, the pressure and the area of the e -th element. To calculate p_{perc} it is sufficient to generate a list in ascending order of pressure and, starting from the lowest values, determining the following:

$$perc F_R = \sum_{e = \text{lif } p(e) > 0}^{N_k < N_e} p_e A_e \quad (7)$$

as N_k is the number of elements necessary to satisfy Equation 7. The pressure of the N_k -th element in the list is exactly p_{perc} .

Load Histories and Boundary Conditions

Load histories consist of six different steps: the pre-tightening torque is assigned to the screws during the first step, simulating the assembly stage. During the second step, a torsional moment equal to approximately 90% of the theoretical slip value is applied to the hub. In the subsequent steps, the torsional moment is maintained and the flexural moment is progressively increased to a value equal to 50% of the corresponding torsional moment applied. Throughout all load steps, circumferential displacement of the nodes of one of the transverse faces of the shaft is inhibited, as is transverse displacement of the node on the axis of the opposite face. This allows the shaft to deform freely without interfering with its internal state of strain.

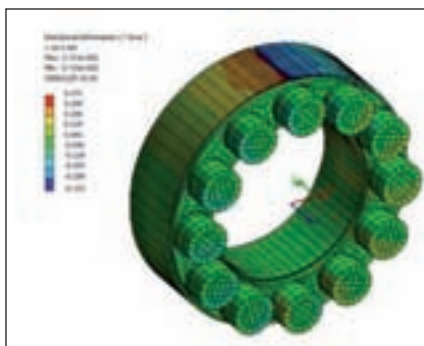


Figure 9—MAV 2005 50 x 80, circumferential displacement of the locking assembly at the end of the pre-tightening stage. The outer ring tends to open, particularly in proximity with the gap, whereas the inner ring in contact with the shaft displays the opposite behavior.

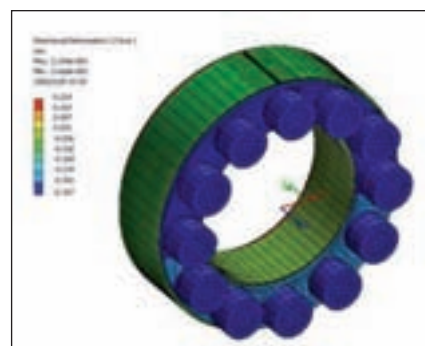


Figure 10—MAV 2005 50 x 80, longitudinal displacement of the locking assembly at the end of the pre-tightening stage. The two conical rings tend to approach one another in a practically symmetrical manner. Overall displacement of the locking mechanism is on the order of a few hundredths of a millimeter.

Results and Conclusions

Tables 4 and 5 give the principle results obtained with the study. In particular, the tables specify the mean pressure values on the shafts, as determined with Equation 6, and the pressure concentration factors, determined with the procedure described previously.

Note how the mean contact pressures for a given measurement vary little with each different load step. This is justified, on the one hand, by the fact that the contact surface remains unaltered (no phenomena of detachment between the locking assembly and shaft ever occur), and, on the other hand, by the fact that as maximum values increase (also by little), this is compensated by an analogous reduction in minimum values. Minimum pressure never assumes values below 30 MPa, ensuring satisfactory adherence between the locking assembly and the shaft, minimizing the risk of fretting.

Note also that an apparently high pressure concentration value, as may be seen with the MAV 1061, is not an indicator of poor locking assembly quality or synonymous with low mechanical performance. The *FCP* must always be evaluated alongside the mean pressure value and maximum transmissible loads, in relation with the effective requisites of the project. This article has briefly described the results obtained using a number of finite element analyses conducted on four different types of locking assembly. The main goal of the exercise was to determine, to a satisfactory degree

of precision, the concentration factor for the contact pressure generated on a shaft by a locking device. The main reasons for the study are the fact that this value cannot be determined by laboratory tests and a scarcity of information available in literature. The results obtained are interesting as they demonstrate that, unexpectedly, peak contact pressure depends very little or not at all on the value of the flexural moment applied, even when the latter reaches values well above those encountered in practice. The reduction in *FCP* with increasing shaft dimensions, a behavior seen practically throughout the entire series, is also very interesting. 

Sandro Zamboni is president of MAV S.p.A.

Massimiliano Margonari is a FEM analysis expert with MAV S.p.A.